NASA
Technical
Paper
2321

May 1984

Intensity and Absorbed-Power Distribution in a Cylindrical Solar-Pumped Dye Laser

M. D. Williams

NASA

NASA
Technical
Paper
2321

1984

Intensity and Absorbed-Power Distribution in a Cylindrical Solar-Pumped Dye Laser

M. D. Williams

Langley Research Center
Hampton, Virginia

NASA
National Aeronautics
and Space Administration

Scientific and Technical
Information Branch

SUMMARY

The pump-source intensity distribution inside a cylindrical dye cell has application to several aspects of dye-laser operation: (1) internal power and energy distribution, (2) lasing and coupling efficiency, (3) thermal and optical performance, and (4) pump-source selection. The main impetus for the work presented here is pump-source selection. Specifically, the internal intensity and absorbed-power distribution of a simplified hypothetical dye laser of cylindrical geometry is calculated. Total absorbed power is also calculated and compared with laboratory measurements of lasing-threshold energy deposition in a dye cell to determine the suitability of solar radiation as a pump source or, alternatively, what modifications, if any, are necessary to the hypothetical system for solar pumping.

INTRODUCTION

NASA research on laser power transmission in space began in 1972 and involved several types of lasers (ref. 1). In the late 1970's the program focused on the use of solar-pumped lasers. Several prospective active media for solar pumping have been identified and investigated in the program. One of these is dye. Dyes offer comparatively good solar spectral absorption, lasing efficiency, excellent tunability, and low cost. However, very large light intensities are required for their operation. A question of prime importance then is whether focused sunlight can pump dye lasers. The theory reported here, although available for broader application, is used with experimental data to provide information relevant to this question.

SYMBOLS

A	area element
A_s	area element of dye-tube surface
C	solar-concentration factor
$E(\lambda)$	solar spectral power distribution
$E'(\theta)$	intensity from a particular direction
E_s	solar constant, W/mm^2
E'_α	absorbed intensity from particular direction
$F(\alpha,R)$	defined in equation (6)
F_f	fluorescent frequency conversion factor
F_g	geometric absorption factor
F_ℓ	length factor

F_m	dye-molecule factor
I	intensity inside cylinder, W/mm^2
I_0	intensity on area element, W/mm^2-sr
n	concentration
P	power emitted into interior, W
P_α	power absorbed from all directions
P'_α	power absorbed from particular direction
R	radius from center of cylinder to dA element
R_0	radius of cylinder, mm
R_1	distance between dA_s and dA, mm
T	Fresnel transmission factor
V	volume
α	dye-absorption coefficient, mm^{-1}
$\alpha(\lambda)$	wavelength-dependent absorption coefficient
γ	angle of solar subtense, radians
θ	angle between R_0 and R, radians
λ	wavelength
λ_1, λ_2	lower and upper bounds of wavelength, respectively
$\sigma(\lambda)$	spectral molecular-absorption cross section
ϕ	angle between R_0 and R_1, radians

MODEL THEORY

A long cylindrical geometry for the dye cell is postulated for the model. The cell is surrounded by an optical concentrator which collects solar radiation in space through a large aperture and directs central rays from the Sun at the cell axis perpendicular to it. The concentrator surface is distant enough from the cell that from any point on the surface of the concentrator, the cell subtends a smaller angle (normal to the cell axis) than that of the solar disc. Such concentrators are possible. Further consideration of the concentrator is not germane to the model presented here. Thus, the dye tube is bathed with uniform concentrated sunlight over its length. At any point on the surface of the dye tube, light is incident through 180° in any plane normal to the tube axis. In all planes containing the tube axis, light is incident at any point on the tube surface at angles of 0° through 0.26° (half the angle of solar subtense γ). With this idealized but feasible geometry, intensity

within the dye cell will have only radial dependence. With term definitions given in figure 1, the equation for intensity within the dye cell can be developed as follows:

With I_0 incident on the area element of the dye-tube surface dA_s, the differential power emitted into the interior is

$$d^2P = I_0 \, dA_s \frac{dA}{R_1^2} \cos \phi \tag{1}$$

The differential intensity at the area element dA in the dye is

$$dI = I_0 T e^{-\alpha R_1} \frac{dA_s}{R_1^2} \cos \phi \tag{2}$$

where

T Fresnel transmission factor

α dye-absorption coefficient, mm^{-1}

$$dA_s = \left(2R_1 \tan \frac{\gamma}{2}\right) R_0 \, d\theta \approx R_1 R_0 \gamma \, d\theta$$

Therefore,

$$dI \approx I_0 T e^{-\alpha R_1} \frac{R_0}{R_1} \cos \phi \, \gamma \, d\theta \tag{3}$$

$$\frac{I}{I_0} \approx 2\gamma R_0 \int_0^{\pi} \frac{T e^{-\alpha R_1}}{R_1} \cos \phi \, d\theta \tag{4}$$

Expressing I_0 in terms of the solar constant E_s and solar-concentration factor C (ref. 2) gives

$$I_0 = \frac{E_s C}{4\pi \sin \frac{\gamma}{2}} \approx \frac{E_s C}{2\pi\gamma} \tag{5}$$

and

$$\frac{I}{E_s C} = \frac{R_0}{\pi} \int_0^{\pi} \frac{Te^{-\alpha R_1}}{R_1} \cos \phi \, d\theta = F(\alpha, R) \tag{6}$$

The following approximations have been included in the derivation:

(1) Scattered light is negligible.

(2) Dimensions of the concentrating optics are much greater than the tube radius.

Now consider a particular radial position in the dye. Rays of light converge there from 360° in a plane normal to the axis. The intensity of any particular ray (denoted by a prime) undergoes a differential absorption in a distance dR_1 given by

$$dE'_{\alpha} = \alpha \, E'(\theta) \, dR_1 \tag{7}$$

The power absorbed from a particular direction is

$$dP'_{\alpha} = A \, dE'_{\alpha} = \alpha \, E'(\theta) \, A \, dR_1 \tag{8}$$

$$\frac{dP'_{\alpha}}{dV} = \alpha \, E'(\theta) \tag{9}$$

Therefore, the differential power absorbed per unit volume from <u>all</u> directions is

$$\frac{dP_{\alpha}}{dV} = \alpha \int_{\theta} E'(\theta) \, d\theta = \alpha E_s C \, F(\alpha, R) \tag{10}$$

Since attenuation is wavelength dependent,

$$\frac{dP_{\alpha}}{dV} = C \int_{\lambda_1}^{\lambda_2} \alpha(\lambda) \, F(\alpha, R) \, \frac{\partial E_s}{\partial \lambda} \, d\lambda = C \int_{\lambda_1}^{\lambda_2} \alpha(\lambda) \, E(\lambda) \, F(\alpha, R) \, d\lambda \tag{11}$$

where $E(\lambda)$ is the solar spectral power distribution.

CALCULATIONS

In equation (6), $F(\alpha,R)$ was evaluated at 21 radial positions (from centerline to periphery, 2 mm) and with 11 dye concentrations (absorption coefficient, 0 to 2 mm^{-1}). (It should be noted that $F(\alpha,R)$ may be normalized to $F(\alpha R_0, R/R_0)$ for application to other laser geometries.) The calculations include assumptions that: (1) the index of refraction of the dye solution is 1.32, (2) the index of refraction of the glass tube enclosing the dye is 1.5, and (3) reflection at the interface of the glass and solution is negligible. Each data point represents the sum of incremental intensities from every direction in a plane normal to the dye-tube axis. The increment used for the summation was 0.5°, which is approximately the angle subtended by the Sun. Actual data values are presented in table I in groups of rows and columns. Each group corresponds to a particular dye-absorption coefficient α; from top to bottom the coefficients are α = 0, 0.2, 0.4, 0.6, ..., 2.0 mm^{-1}, respectively. Within each group the value in the upper left corner is the normalized intensity at the dye-tube centerline ($R/R_0 = 0$). Successively larger values of R/R_0 (0.05, 0.10, 0.15, ...) are read from left to right, top to bottom, in each group.

The data of table I are plotted in figure 2. The top curve corresponds to $\alpha = 0$ (no dye present). Successively lower curves correspond to α = 0.2 through 2.0 mm^{-1}.

Spectral values of $\alpha(\lambda)$ and $E(\lambda)$ were taken from references 3 and 4, respectively, and used with values of $F(\alpha,R)$ interpolated from table I to calculate absorbed-power density dP_α/dV at 21 radial positions. Figure 3 shows dP_α/dV plotted against radial position R/R_0. From top to bottom, the curves correspond to 4n, 2n, n, and n/2, respectively, where the concentration n is 1.51×10^{13} molecules per cubic millimeter, the dye concentration of the experiment discussed in the appendix. (Here, $\alpha(\lambda)$ varies with n according to $\alpha(\lambda) = n\,\sigma(\lambda)$, where $\sigma(\lambda)$ is the spectral molecular-absorption cross section.)

The absorbed-power density dP_α/dV integrated over the volume of the tube gives the total power absorbed by the dye. The integration was performed numerically for all curves of figure 3 and was evaluated at various dye concentrations as follows:

Concentration	Power, W
n/2	0.02623C
n	.038C
2n	.052C
4n	.066C

DISCUSSION

The curves of $F(\alpha,R)$ in figure 2 show expected trends at the centerline and boundary of the dye. At the centerline ($R/R_0 = 0$), intensity decreases exponentially according to

$$F(\alpha,0) = Te^{-\alpha R_0} \tag{12}$$

as dye concentration n increases. This is caused, of course, by higher concentrations of dye absorbing more light in the outer portions of the dye before the light can reach the center of the tube. The integral form of the normalized intensity (see eq. (6)) reduces exactly to the exponential form in equation (12) at the centerline where $R_1 = R_0$, $T = 0.96$, and $\phi = 0$. At the outer boundary ($R/R_0 = 1$) the integral equation does not reduce to a simple form, but there is a more rapid attenuation toward an intensity limit which is determined by the amount of light that can be gathered through the tube wall. (In the limit as α becomes very large, negligible light would come from the dye side of the outer boundary.) Calculations of the intensities at the outer boundary were not done because of time limitations associated with the computer program. Rather, those intensities were extrapolated from the nearest three data points of each curve.

At radial positions between the two extremes, the most notable feature is the abrupt intensity decrease near $R/R_0 = 0.7$. That feature is caused by Fresnel reflection at the surface of the glass tube. At these radial distances a range of θ values exists for which the corresponding refraction angles are impossible, meaning that no light can reach some of the larger radial positions from some points on the surface of the dye tube. The greater the radial position, the greater these "blind" and "nearly blind" areas are on the tube surface.

The data of table I are sufficient to interpolate $F(\alpha,R)$ for α values only as large as 2. This limits the number of curves in figure 3. If more curves had been calculated, their character would vary approximately as indicated in figure 4; that is, values near the centerline would begin to decrease, and values at the boundary would continue to increase.

None of the curves of figure 3 have zero slope over extended lengths. This means that there is no absolutely uniform energy deposition over large areas. (Absolute uniform deposition is achieved only for the trivial case where there is no energy deposition at all.) This indicates that a radial thermal gradient will always exist in such a laser volume with such irradiation. Gradient magnitudes will vary during illumination until an equilibrium is established and will cause variations in the refractive index of the fluid which, in turn, cause lenslike effects in the optical cavity that can destroy optical feedback. Longer cavities are more sensitive to the gradients if other laser parameters remain unchanged. The growth rate of the gradients can be lessened by smaller dye concentrations, in which case a longer length is needed to compensate for loss of optical gain. Steady-state gradients could be minimized by optically designing solar radiation to be focused more toward the center of the tube. If, simultaneously, dye concentration were increased, total power deposition would be increased.

The absorbed-power density dP_α/dV integrated over the cylindrical volume of the dye was evaluated previously. This information may be combined with data from our laboratory dye-laser system (see the appendix) to provide an estimate of the solar-concentration factor required to operate a solar-pumped dye laser (like our laboratory system) in space.

If this same laboratory laser were illuminated in space as our model theory describes, the total power absorption as calculated from theory approximates the absorbed power that was measured in the laboratory (26 700 W) in order to reach

lasing threshold. From this relationship an estimate of the solar concentration required to reach lasing threshold is

$$C = \frac{26\ 700}{0.038} \approx 7 \times 10^5$$

This is about 35 times the maximum geometrical solar concentration attainable in practice. (The Sun does not approximate a point source well enough to achieve practical concentrations greater than 20 000.) Therefore, a feasible model must incorporate improvements that compensate for the factor 35 while maintaining a solar concentration of 20 000. Improvements can take several forms, some of which are stated as follows: (1) absorption by the dye mixture can be made more efficient both geometrically and spectrally, (2) fluorescent frequency conversion may be used, (3) the rhodamine-dye molecule may be improved, and (4) laser-gain length can be increased. Each of these possible improvements will be addressed briefly.

Recall the absorbed powers calculated previously. These data may be extrapolated to very high dye densities to show that absorbed power may be increased by a factor of 1.7 by increasing dye concentration. Conversely, this same factor could be gained geometrically by multipass absorption in the same dye concentration rather than by the single-pass absorption of the model. This factor is labeled the "geometric absorption factor" F_g.

Outside the absorption band of all dyes, fluorescent frequency conversion could also be used to translate incoming radiation into absorption bands (refs. 5 and 6). (Fluorescent frequency conversion may be viewed as nongeometric solar concentration.)

From a theoretical treatment of dye-laser threshold, reference 7 shows that the lasing threshold of the rhodamine 6G molecule cannot be reduced by more than a factor of 4. This reference also shows that self-tuned critical inversion is inversely proportional to the three-fourths power of laser length (if triplet population is kept small and/or cavity losses are sufficiently large).

The product of the aforementioned factors must be greater than 35. That is,

$$F_g F_f F_m F_\ell > 35$$

where

F_f fluorescent frequency conversion factor

F_m dye-molecule factor

F_ℓ length factor

If we estimate the factors as follows:

$$F_g = 1.5 \qquad F_f = 3 \qquad F_m = 1$$

and

$$F_{\ell} > \frac{35}{4.5} = 7.77$$

then F_{ℓ} would correspond to a length change by a factor of 15.41. That is, the active length of the model laser system must be 4.72 m to achieve a lasing threshold. It is practically impossible to build a solar concentrator that will provide the radiation geometry of this lengthened model at a solar concentration of 20 000. Therefore, it is not possible to build a solar-pumped dye laser of this particular lengthened geometry in practice. However, another geometry that provides the increased length (with essentially the same laser cavity and absorbed-power density) might be possible, assuming, of course, that threshold-length scaling actually follows theoretical predictions at the required length.

CONCLUDING REMARKS

The intensity and power distribution inside a cylindrical dye cell have been calculated and presented in normalized form for application to a model system and to other similar systems. Also, the relevant equations were derived and presented for use on systems with major geometrical differences (e.g., nonuniform illumination). These equations and calculations serve as a basis for investigations into other areas of dye-laser research, such as thermal, thermo-optical, modal, and optical analyses.

For the particular space-based model examined here, analysis shows that radial gradients in absorbed-power deposition exist and increase with dye concentration. (Radial gradients cause lenslike effects deleterious to lasing.) Total-power deposition also increases, which suggests the existence of an "optimum" optical geometry wherein radial gradients are minimized and total-power deposition is maximized. Such an optimum geometry might be achieved by increasing dye concentration and focusing solar radiation more toward the center to compensate for attenuation in outer regions of the tube. This calls for a particular concentrator design for each particular dye concentration and geometry, and the resultant distribution of power deposition would be valid only for the unique directional, spectral, and emissive properties of the Sun.

Calculations show quantitatively that improvements on the postulated model are necessary to reach lasing threshold. Several possible improvements are identified and their effects are estimated from data here and in referenced literature. The effects are estimated conservatively and indicate that the active length of the model laser system must be 4.72 m (at a solar concentration of 20 000) to achieve lasing threshold. Since it is not possible to achieve the required solar concentration over the required length in practice, it is not possible to build a solar-pumped laser with the geometry of the model. Another geometry that provides the required length and concentration (with essentially unchanged laser-cavity characteristics) might be possible if lasing threshold actually varies with length as theory predicts.

Langley Research Center
National Aeronautics and Space Administration
Hampton, VA 23665
April 11, 1984

APPENDIX

LABORATORY MEASUREMENTS OF DYE-LASER MODEL

The laboratory laser model consisted of a xenon flash lamp and dye-laser tube housed inside an almost cylindrical reflective cavity. (Actually, the cavity cross section was an almost circular ellipse with the laser tube at one focus and the flash lamp at the other focus.) The flash lamp was driven by a capacitive network which simulated a transmission line and produced an approximate square wave current pulse of 1-msec duration. The network was charged to voltages as large as 5 kV and was triggered by a pulse transformer connected in series with the lamp.

Rhodamine-dye solution was circulated in series through a pump, connection tubes, laser tube, reservoir, and filter. All materials contacting the dye were Teflon,[1] stainless steel, and glass, except for the commercially available filter material that was unknown.

The laser tube was a cylindrical Pyrex[2] glass tube 304.8 mm long with an inside diameter of 4.0 mm and an outside diameter of 6.35 mm filled with rhodamine 590, methanol, water, and cyclo-octatetraene, an effective triplet-state quencher. The output mirror was 1 percent transmissive, the rear mirror was almost totally reflective, and both had a 10-m radius of curvature. Dye concentration was 1.51×10^{13} molecules per cubic millimeter.

Energy absorbed by the dye solution was determined from volumetric expansion of the solution after a flash-lamp pulse and was found to be approximately 26.7 J. Thus, absorbed power during the 1-msec pulse was approximately 26 700 W. (Subsequent measurements with an improved system indicate that the absorbed power can be reduced by almost a factor of 2.)

[1]Teflon: Trademark of E. I. du Pont de Nemours & Co., Inc.
[2]Pyrex: Trademark of Corning Glass Works.

REFERENCES

1. Williams, M. D.; and Conway, E. J., eds.: Space Laser Power Transmission System Studies. NASA CP-2214, 1982.

2. Meinel, Aden B.; and Meinel, Marjorie P.: Applied Solar Energy - An Introduction. Addison-Wesley Pub. Co., Inc., c.1976.

3. Snavely, B. B.: Continuous-Wave Dye Lasers. Dye Lasers, Second rev. ed., F. P. Schäfer, ed., Springer-Verlag Berlin Heidelberg, 1977, pp. 86-120.

4. Sayigh, A. A. M., ed.: Solar Energy Engineering. Academic Press, 1977.

5. Moeller, C. E.; Verber, C. M.; and Adelman, A. H.: Laser Pumping by Excitation Transfer in Dye Mixtures. Appl. Phys. Lett., vol. 18, no. 7, Apr. 1, 1971, pp. 278-280.

6. Wladimiroff, W. W.: Some Stable Fluorescent Converter Solutions Enhancing Optical Pumping in the Visible Region. Photochem. & Photobiol., vol. 6, 1967, pp. 543-556.

7. Peterson, O. G.; Webb, J. P.; McColgin, W. C.; and Eberly, J. H.: Organic Dye Laser Threshold. J. Appl. Phys., vol. 42, no. 5, Apr. 1971, pp. 1917-1928.

TABLE I.- INTENSITY VALUES

α, mm^{-1}	Intensity values $F(\alpha,R)$ at increments of R/R_0						
0	0.9600	0.9600	0.9600	0.9600	0.9600	0.9599	0.9598
	.9596	.9593	.9587	.9577	.9561	.9530	.9470
	.9334	.8761	.7133	.6375	.5832	.5380	.5019
0.2	0.6435	0.6437	0.6444	0.6455	0.6472	0.6492	0.6516
	.6546	.6579	.6617	.6657	.6699	.6737	.6761
	.6735	.6381	.5196	.4666	.4296	.3984	.3730
0.4	0.4314	0.4317	0.4329	0.4349	0.4376	0.4412	0.4456
	.4508	.4569	.4639	.4718	.4804	.4895	.4984
	.5044	.4861	.4023	.3676	.3447	.3256	.3103
0.6	0.2891	0.2896	0.2911	0.2935	0.2969	0.3013	0.3068
	.3134	.3211	.3301	.3403	.3518	.3644	.3778
	.3899	.3842	.3271	.3068	.2952	.2860	.2792
0.8	0.1938	0.1943	0.1958	0.1984	0.2020	0.2067	0.2126
	.2197	.2281	.2380	.2494	.2624	.2770	.2930
	.3092	.3127	.2759	.2666	.2642	.2631	.2633
1.0	0.1299	0.1304	0.1319	0.1344	0.1379	0.1425	0.1483
	.1553	.1638	.1737	.1854	.1988	.2143	.2317
	.2502	.2601	.2386	.2380	.2430	.2488	.2554
1.2	0.0871	0.0875	0.0889	0.0912	0.0944	0.0987	0.1040
	.1107	.1186	.1282	.1394	.1527	.1681	.1859
	.2056	.2199	.2099	.2161	.2269	.2388	.2518
1.4	0.0584	0.0588	0.0599	0.0619	0.0648	0.0686	0.0734
	.0794	.0867	.0954	.1060	.1185	.1334	.1510
	.1710	.1881	.1868	.1982	.2140	.2312	.2498
1.6	0.0391	0.0395	0.0405	0.0422	0.0446	0.0479	0.0521
	.0573	.0638	.0717	.0813	.0929	.1069	.1237
	.1435	.1623	.1674	.1829	.2028	.2247	.2485
1.8	0.0262	0.0265	0.0273	0.0287	0.0308	0.0335	0.0371
	.0416	.0472	.0542	.0628	.0733	.0863	.1022
	.1213	.1410	.1508	.1694	.1928	.2190	.2479
2.0	0.0176	0.0178	0.0185	0.0196	0.0213	0.0236	0.0266
	.0304	.0352	.0412	.0488	.0582	.0701	.0848
	.1031	.1230	.1362	.1573	.1836	.2137	.2476

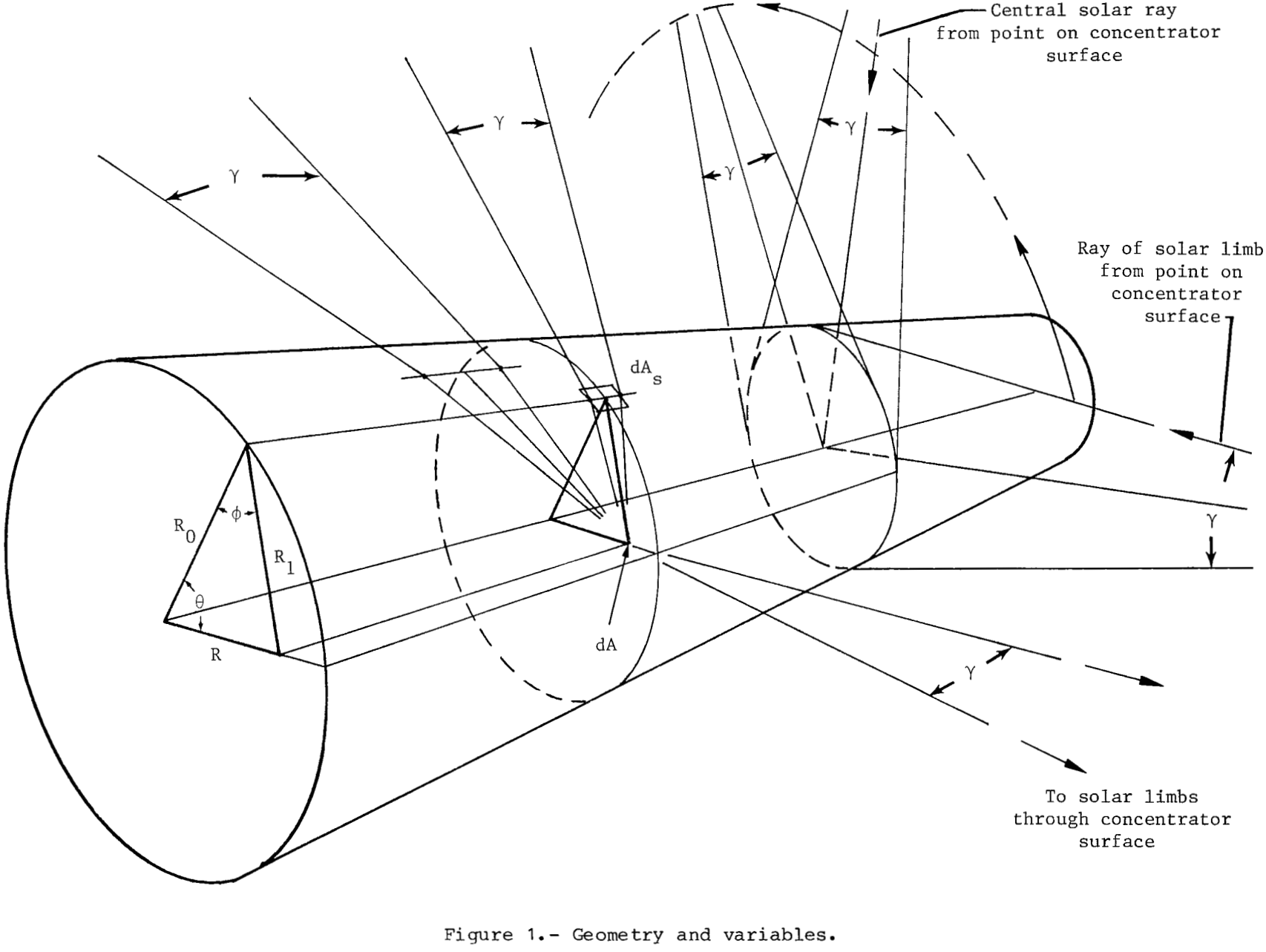

Figure 1.- Geometry and variables.

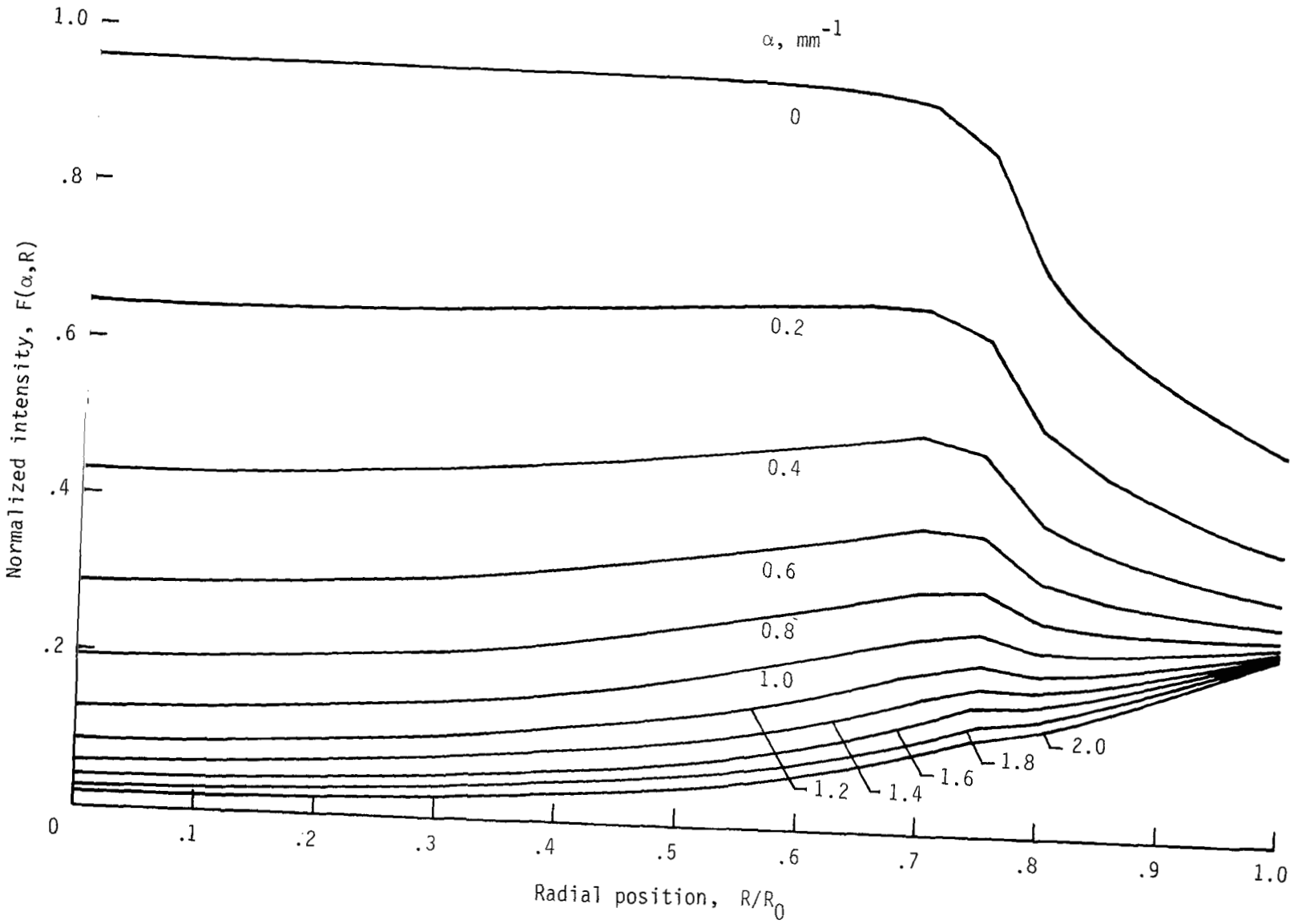

Figure 2.- Intensity distribution in dye.

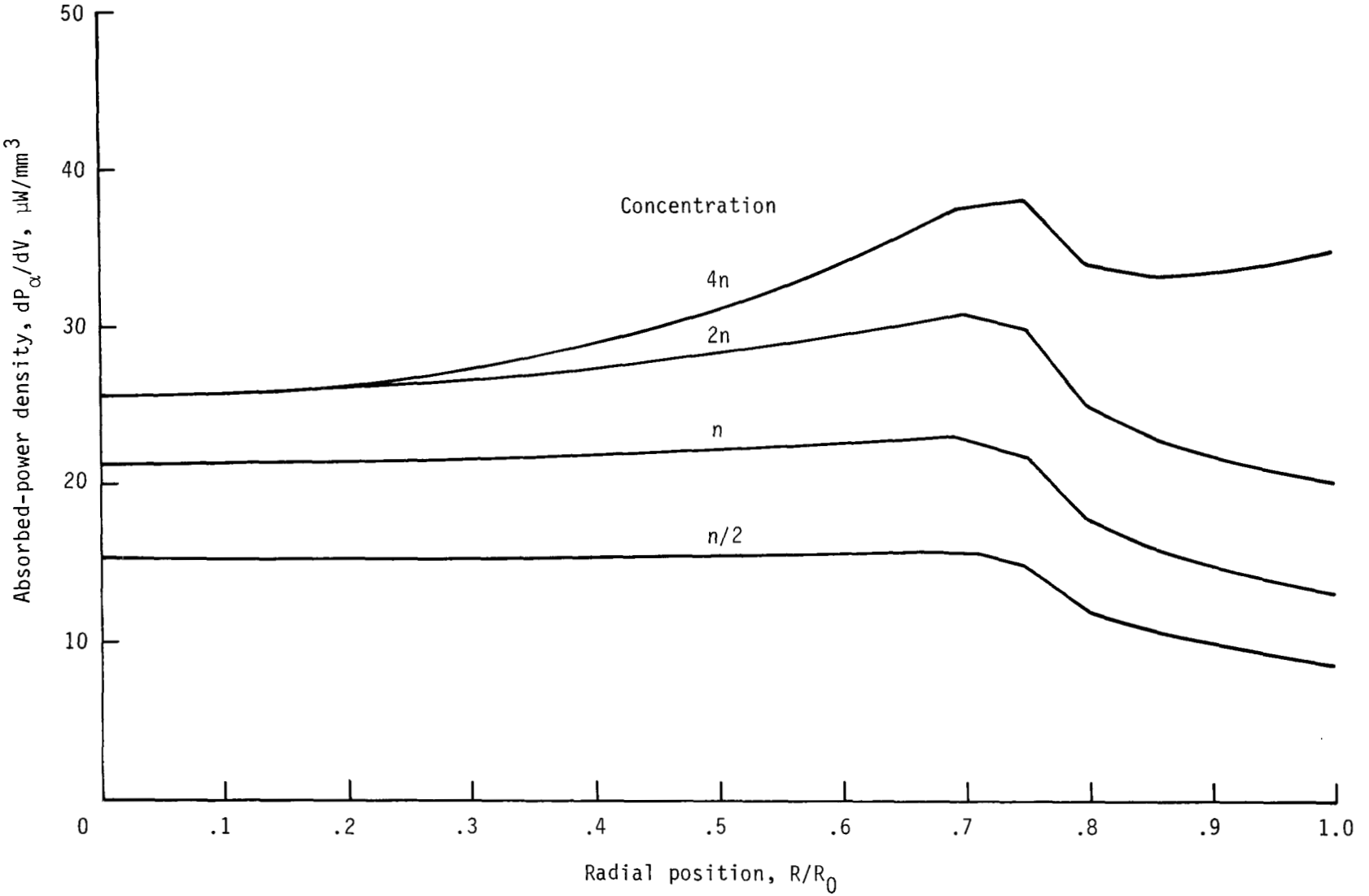

Figure 3.- Absorbed-power density in dye.

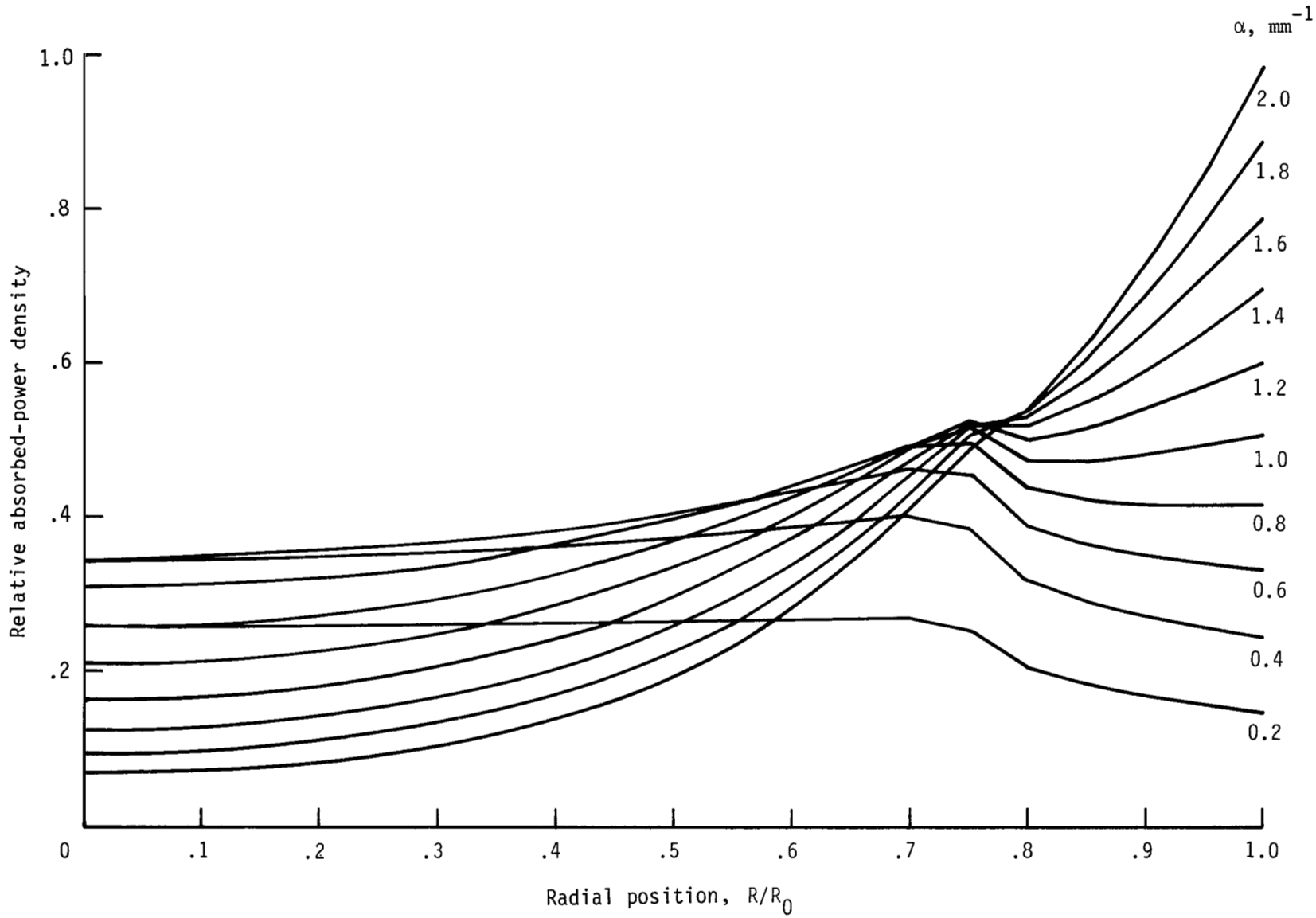

Figure 4.- Trend of absorbed-power density at larger dye concentrations.

1. Report No.	2. Government Accession No.	3. Recipient's Catalog No.
NASA TP-2321		

4. Title and Subtitle	5. Report Date
INTENSITY AND ABSORBED-POWER DISTRIBUTION IN A CYLINDRICAL SOLAR-PUMPED DYE LASER	May 1984
	6. Performing Organization Code: 506-55-73-01
7. Author(s): M. D. Williams	8. Performing Organization Report No.: L-15694
	10. Work Unit No.
9. Performing Organization Name and Address: NASA Langley Research Center, Hampton, VA 23665	11. Contract or Grant No.
	13. Type of Report and Period Covered: Technical Paper
12. Sponsoring Agency Name and Address: National Aeronautics and Space Administration, Washington, DC 20546	14. Sponsoring Agency Code

15. Supplementary Notes

16. Abstract

The internal intensity and absorbed-power distribution of a simplified hypothetical dye laser of cylindrical geometry is calculated. Total absorbed power is also calculated and compared with laboratory measurements of lasing-threshold energy deposition in a dye cell to determine the suitability of solar radiation as a pump source or, alternatively, what modifications, if any, are necessary to the hypothetical system for solar pumping.

17. Key Words (Suggested by Author(s))	18. Distribution Statement
Dye lasers Solar pumping Energy conversion	Unclassified - Unlimited Subject Category 36

19. Security Classif. (of this report)	20. Security Classif. (of this page)	21. No. of Pages	22. Price
Unclassified	Unclassified	16	A02

For sale by the National Technical Information Service, Springfield, Virginia 22161 NASA-Langley, 1984

2 1 1U,D, 840511 S00916DS
DEPT OF THE AIR FORCE
AF SYSTEMS COMMAND
ATTN: AFSC LIAISON OFFICE MS 221
NASA LANGLEY RESEARCH CENTER
LANGLEY AFB VA 23665